Modelling Calibration and Validation of Contributions to Stress in the STI Process Sequence[1]

K. Garikipati[†], V.S. Rao[‡], M.Y. Hao[§], E. Ibok[¶] I. De Wolf[‖], R.W. Dutton[**]

[†]Center for Integrated Systems, Stanford University, CA, USA, krishna@gloworm.stanford.edu
[‡]Schlumberger Cambridge Research Centre, Cambridge, UK, rao@cambridge.scr.slb.com
[§]Advanced Micro Devices, Santa Clara, CA, myhao@amd.com
[¶]Advanced Micro Devices, Santa Clara, CA, effiong.ibok@amd.com
[‖]Interuniversity Micro-electronics Center, Leuven, Belgium, dewolfi@imec.be
[**]Center for Integrated Systems, Stanford University, CA, USA, dutton@gloworm.stanford.edu

ABSTRACT

The mathematics and mechanics of the Shallow Trench Isolation process are described. The diffusion-reaction problem is posed in terms of fundamental mass balance laws. Finite strain kinematics is invoked to model the large expansion of SiO_2, dielectrics are modelled as viscoelastic solids and annealing-induced density relaxation of SiO_2 is incorporated as a history-dependent process. A levelset framework is used to describe the moving Si/SiO_2 interface. Sophisticated finite element methods are employed to solve the mathematical equations posed for each phenomenon. Mechanical properties of viscoelastic solids are extracted directly from stress-strain data, following which, parameters for the diffusion-reaction problem are obtained. Comparison with micro-Raman spectroscopy provides validation of the model.

Keywords: mathematical modelling, continuum mechanics, viscoelasticity, semiconductor processing, finite element methods.

1. INTRODUCTION

Isolation structures are employed in IC technology to provide insulation between current-carrying Silicon regions. The processing sequence involves steps such as etching away of material, deposition of new material, diffusion of Oxygen, oxidation, moving interfaces between Silicon and Silicon dioxide, and the mechanics associated with large volume changes. Some of these steps are carried out at temperatures in the range of $900^\circ - 1000^\circ$C. The profiles assumed by various materials, their interfaces, the stress generated during the process and residual stress at the end, all affect the electrical characteristics of the device. Additionally, nucleation of dislocations in Silicon results in catastrophic degeneration of electrical performance. Clearly, accurate modelling of stress is of crucial importance to prediction of device performance.

2. MATHEMATICS AND MECHANICS

The mathematical models are rigorously based on continuum mechanics [1].

[1]Partially supported by AMD Inc., Santa Clara.

2.1 Diffusion-Reaction

The diffusion-reaction problem is treated on the basis of mass balance laws. A Rankine-Hugoniot relation is arrived for the velocity of the moving Silicon/Silicon dioxide interface.

$$V_n = -\frac{[\![\boldsymbol{T}_{\rm ox}\cdot\boldsymbol{n}]\!]}{[\![\rho_{\rm ox}]\!]}. \tag{1}$$

In the above equation, V_n is the normal interface velocity, $\boldsymbol{n}$ is the normal to the interface, $\boldsymbol{T}_{\rm OX}$ is the flux of SiO_2, $\rho_{\rm OX}$ is the concentration of SiO_2 and $[\![\cdot]\!]$ represents a jump in the corresponding quantity. A levelset formulation has been employed to treat the moving interface by introducing the function $\varphi(\boldsymbol{x},t)$ which represents the signed distance of a point from the Si/SiO_2 interface. This results in a nonlinear advection equation that can be defined over the entire problem domain.

$$\frac{\mathrm{d}\varphi}{\mathrm{d}t} = \frac{\partial\varphi}{\partial t} - V_n\|\nabla\varphi\| = 0. \tag{2}$$

At points away from the interface, the velocity of levelset contours is obtained via a closest point projection. The interface is allowed to pass through elements and separates the domain into Silicon and Silicon dioxide regions. The concentration and flux of O_2 are discontinuous across the interface and are governed by

$$\nabla\cdot(D\nabla\rho) = 0, \tag{3}$$

where D is the diffusivity which is a function of stress: $D = D_0\exp(-pV_d/kT)$, with p being the hydrostatic pressure.

2.2 Mechanics

The newly formed Silicon dioxide instantaneously expands to a stress-free volume that is 2.2 times that of Silicon. Finite strain kinematics are invoked to model the accompanying mechanics thus introducing nonlinear strain measures such as the Right Cauchy-Green stretching tensor, $\boldsymbol{C}$ [1]. This expansion is constrained by surrounding material. The stress that arises thereby is modelled at the constitutive level within a neo-Hookean stored energy function $\psi(\boldsymbol{C})$, via the relation

$$\boldsymbol{S} = 4\frac{\partial\psi(\boldsymbol{C})}{\partial\boldsymbol{C}}. \tag{4}$$

The Standard-Solid Viscoelastic Model (Figure 1) has been adopted for the oxide and other dielectrics.

Silicon dioxide, when annealed at temperatures greater than 650°C, demonstrates a complex, time dependent density relaxation which is parametrized by temperature. The associated stress-free expansion has been phenomenologically treated via an internal variable formulation [2].

$$\vartheta(t) = \frac{(n_0-1)^\alpha}{(n_\infty - 1 + (n_0 - n_\infty)\exp[-(t/\tau)^a])^\alpha} \quad (5)$$

$$\bar{\tau}(T) = \bar{\tau}_0 \exp(E_A/kT) \quad (6)$$

$$\bar{\tau}_0 = 1.26 \times 10^{-21}\text{s} \quad (7)$$

$$E_A = 6\text{eV}. \quad (8)$$

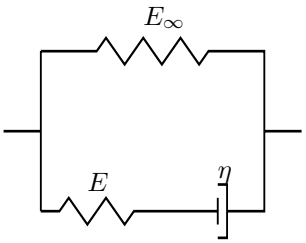

Figure 1: Schematic representation of the Standard Solid Viscoelastic Model for the one dimensional case

The volumetric expansion ratio is $\vartheta(t)$, n is the refractive index and subscripts $(\cdot)_0$ and $(\cdot)_\infty$ refer to initial and final values of the corresponding quantities. Suitable values of the exponents are $\alpha = 0.17$ and $a = 1.63$.

Plane strain conditions [3] are throughout assumed for the mechanics.

3. NUMERICAL METHODS

Advanced finite element methods have been developed for the numerical solution of the mathematical models mentioned above [2]. The Oxygen concentration develops a discontinuity across the Silicon/Silicon dioxide interface. The governing differential equation for diffusion therefore must admit discontinuities. Numerically, these are treated in the setting of "enhanced gradient" finite element methods to allow discontinuous fields within an element (see Figure 2).

The nonlinear advection equation requires numerical stabilization, which is provided by taking recourse to the Galerkin Least Squares formulation [4].

The Silicon dioxide region in an element containing the interface has a stress-free volume that is 2.2 times that of Silicon in the remaining part of the element. This highly inhomogeneous expansion is treated in the context of enhanced strain finite element methods [5].

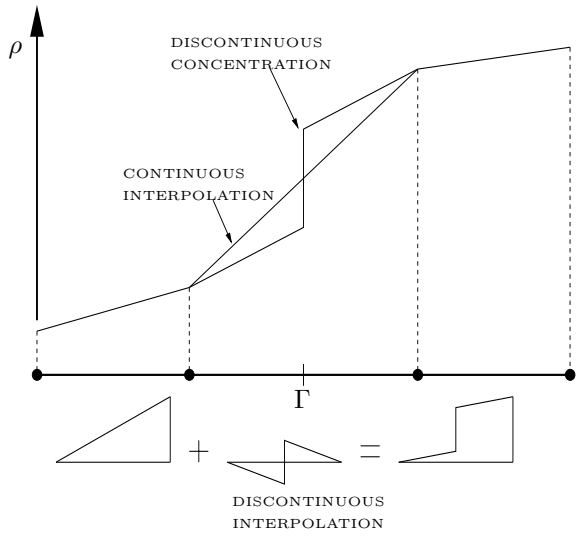

Figure 2: Example of one-dimensional diffusion with discontinuity in concentration across an interface, Γ. Note that the interface lies within the element and that concentration is continuous across elements.

4. PARAMETER EXTRACTION

The mechanical parameters appearing in the viscoelastic material model have been determined by fitting to the stress-relaxation data of Yu et al. [6]. Figure 3 demonstrates that the viscoelastic behavior of SiO_2 is indeed represented very well by the Standard Solid Model.

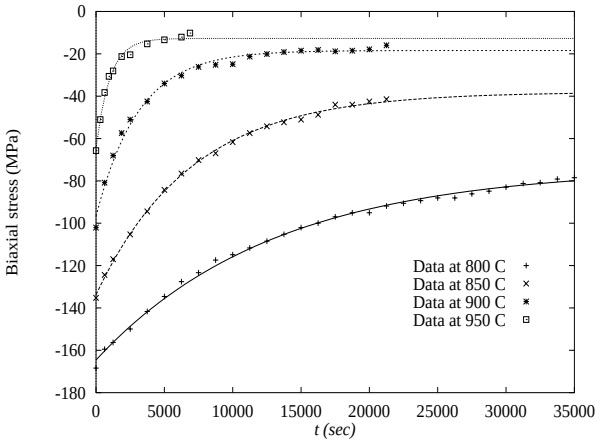

Figure 3: Fits to the isothermal relaxation data of Yu et al. using the standard solid viscoelastic model. The oxide was thermally grown dry at 1150° C and subsequently annealed at the indicated temperatures.

Following this step, the growth parameters, V_d, V_r, D_0 and k_{s0} are obtained by running the code and adjusting these parameters to fit Kao's [7] growth data. Importantly, the mechanical parameters are unaffected by the

choice of growth parameters. This is to be contrasted with the situation in certain earlier works [8], [9], where mechanical quantities such as activation volume for viscosity are determined by fitting to growth data.

5. VALIDATION AND NUMERICAL EXAMPLES

The aim of this section is to demonstrate the validity of the models introduced. At issue is the correct representation of stress in qualitative and quantitative terms. Qualitative aspects will be demonstrated by attainment of the proper sign of stress components in STI process sequences. Micro-Raman stress measurements provide validation of the models in terms of the actual stress values calculated.

5.1 Computation of stress in an STI process

A numerical example is presented to demonstrate calculations for the entire STI process. A portion of a test structure consisting of an array of alternating long lines and trenches is considered. Symmetry is employed to carryout the solution over the half-width of a line and adjoining trench. The actual line and trench are each 4μm wide. The trench is 0.35μm deep. Each stage of the process is solved for, accounting for thermal oxidation, deposition or removal of material and the accompanying mechanics. Some key stages in the process are depicted in Figures 4-7.

5.2 Validation of STI stress

This section presents a comparison between micro-Raman Spectroscopy measurements and a numerical solution of the full STI process sequence upon the portion of the test structure described in Section 5.1. The interested reader is directed to the work of de Wolf and coworkers [10] and references therein for details.

The trends seen in the numerical solutions in Figures 8 and 9 match well with experiment. They indicate compressive stress in the line, changing sharply to tensile under the trench. (The relation between shift in the micro-Raman spectrum and stress is $\sigma_{11} \approx -0.5 \times 10^9 \Delta\omega$, where σ_{11} is the normal stress in the horizontal direction in Figures 8 and 9.) Also, the stress at the end of gate oxidation is lower than that at the end of liner oxidation. This is mainly on account of removal of the nitride mask whose tendency to shrink imposes high compressive stress on the underlying Si substrate. In contrast, the expansion of SiO_2 in the trench does not pose as much of a compressive stress in the adjacent line. The mismatch over the active area at the end of gate oxidation appears to be an artifact of modelling the expansion of thermal oxide in a two-dimensional framework. In contrast, the actual test structure, while consisting of long lines, still has three-dimensional expansion of thermal oxide. This comparison would benefit from a fully three-dimensional model.

6. CONCLUSIONS

The formalism of continuum mechanics and accompanying balance laws has been brought to to bear upon the problem. Finite strain kinematics has been argued for and applied in modelling the large expansion of SiO_2. Various experimentally observed phenomena that contribute to the mechanics of the problem have been accounted for in a rigorous manner. The computational methods employed are capabile of calculating the stress at each step of the process. Qualitative and quantitative validation of the models has been presented.

References

[1] J.E. Marsden and T. J. R. Hughes. *Mathematical Foundations of Elasticity*. Dover, New York, 1994.

[2] J. Lubliner. *Plasticity Theory*. MacMillan, 1990.

[3] S. Timoshenko and J. N. Goodier. *Theory of Elasticity*. McGraw-Hill, 1951.

[4] A.N. Brooks and T.J.R. Hughes. Streamline upwind/Petrov-Galerkin formulations for convection dominated flows with particular emphasis on the incompressible Navier-Stokes equations. *Comp. Methods in Applied Mech. Engrg.*, 32:199–259, 1982.

[5] J.C. Simo and M.S. Rifai. A class of mixed assumed strain methods and the method of incompatible modes. *Int. J. Numer. Methods Engrg.*, 29:1595–1638, 1990.

[6] C.L. Yu, P.A. Flinn, and J.C. Bravman. In-situ stress measurements during dry oxidation of silicon. In J.E. Sanchez R.R. Keller, K.S. Krisch and Z. Suo, editors, *Materials Reliability in Microelectronics VII*, pages 95–100. Materials Res. Soc., 1997.

[7] D-B. Kao. *Two Dimensional Oxidation Effects in Silicon – Experiments and Theory*. PhD thesis, Stanford University, June 1986.

[8] C.S. Rafferty. Stress effects in silicon oxidation-simulation and experiments. *Ph.D. Thesis, Stanford University*, 1989.

[9] V. Senez, D. Collard, P. Ferreira, and B. Baccus. Two-dimensional simulation of local oxidation of silicon: Calibrated viscoelastic flow analysis. *IEEE Trans. Electron Dev.*, 43(8):720–730, 1996.

[10] I. de Wolf. Micro-Raman spectroscopy to study local mechanical stress in silicon integrated circuits. *Semicond. Sci. Technol.*, 11:139–154, 1996.

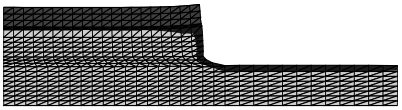

Figure 4: Materials after liner oxidation: Substrate (light grey), barrier/liner oxide (dark grey) and nitride mask (medium grey)

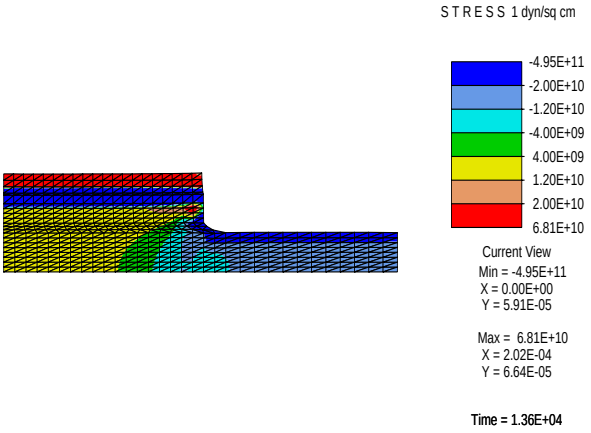

Figure 5: σ_{11} at the end of liner oxide growth

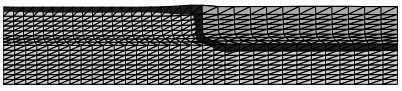

Figure 6: Materials after growth of gate oxide: Substrate (light grey), barrier/liner oxide (dark grey) and filler (medium grey)

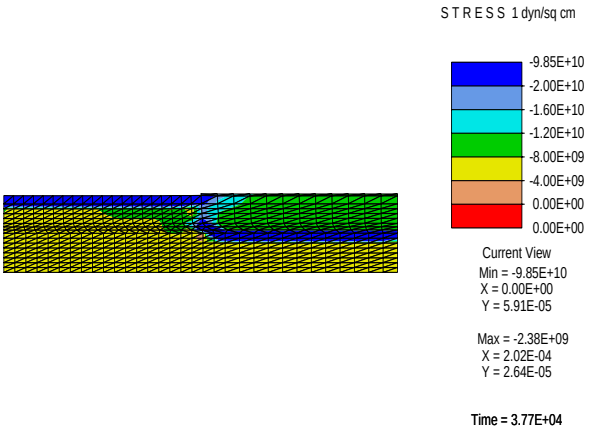

Figure 7: σ_{11} at the end of gate oxide growth

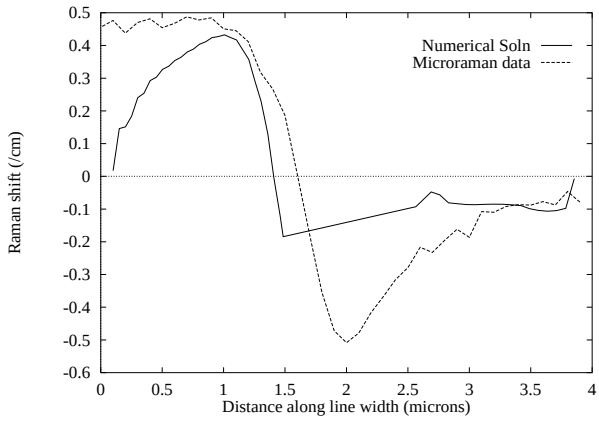

Figure 8: Shift in bandwidth $\Delta\omega$ ($cm^{-}1$) at the end of liner oxidation

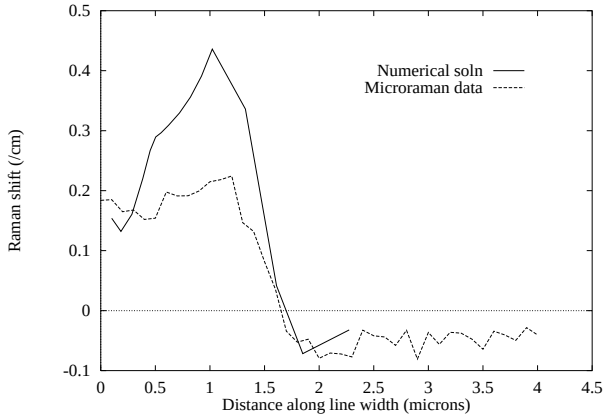

Figure 9: Shift in bandwidth $\Delta\omega$ ($cm^{-}1$) at the end of gate oxidation